GSA Data Repository Item 2017376
Konhauser, K.O., Robbins, L.J., Alessi, D.S., Flynn, S.L., Gingras, M.K., Martinez, R.E., Kappler, A., Swanner, E.D., Li, Y.-L., Crowe, S.A., Planavsky, N.J., Reinhard, C.T., and Lalonde, S.V., 2017, Phytoplankton contributions to the trace element 1 composition of Precambrian banded iron formation: GSA Bulletin, https://doi.org/10.1130/B31648.1.

Supplementary Information for:

Phytoplankton contributions to the trace element composition of Precambrian banded iron formation

Kurt O. Konhauser[1], Leslie J. Robbins[1], Daniel S. Alessi[1], Shannon L. Flynn[1], Murray K. Gingras[1], Raul E. Martinez[2], Andreas Kappler[3], Elizabeth D. Swanner[4], Yi-Liang Li[5], Sean A. Crowe[6], Noah J. Planavsky[7], Christopher T. Reinhard[8] and Stefan V. Lalonde[9]

[1]Department of Earth and Atmospheric Sciences, University of Alberta, Edmonton, AB T6G 2E3, Canada

[2]Institut für Geo- und Umweltnaturwissenschaften, Albert-Ludwigs-Universität, Mineralogie-Geochemie, 79104 Freiburg, Germany

[3]Geomicrobiology, Center for Applied Geosciences, University of Tübingen, 72074 Tübingen, Germany.

[4]Department of Geological and Atmospheric Sciences, Iowa State University, Ames, IA, 50011, USA

[5]Department of Earth Sciences, the University of Hong Kong, Hong Kong

[6]Department of Microbiology and Immunology and Department of Earth, Ocean, and Atmospheric Sciences, University of British Columbia, Vancouver, British Columbia, Canada.

[7]Department of Geology and Geophysics, Yale University, New Haven, CT 06511, USA

[8]School of Earth and Atmospheric Sciences, Georgia Institute of Technology, Atlanta, GA 30332, USA

[9]European Institute for Marine Studies, CNRS-UMR6538 Laboratoire Domaines Océaniques, Technopôle Brest-Iroise, 29280 Plouzané, France

Adsorption Calculation Sensitivity

Adsorption calculations were performed as outlined in the methodology of the main text. Briefly, by calculating the number of deprotonated carboxyl sites at pH 8, and combining this with the extrapolated metal binding constants and initial trace metal concentrations, we were able to determine the amount of each trace metal of interest bound per mg of *R. iodosum* biomass. These calculations, outlined in Table S4, were performed for three separate initial seawater conditions (Table S2) to text sensitivity to the initial seawater composition. The amount of trace metals adsorbed per weight of biomass (μmol mg^{-1}) for the three different initial seawater conditions are provided in Table S4 and Figure S1A. Figure S1A highlights an inherent sensitivity to the initial seawater conditions, which is not entirely unexpected. However, when considered in light of the assimilated trace metals (main text, Table 1) and when carried through our calculations, only minor differences are noticeable in the overall flux of trace metals on a yearly basis (Figure S2); the only major divergence is for Cd when the initial concentration is stoichiometrically fixed to *R. iodosum* and 9 nM Ni. Figure S2 is produced by using the μmol mg^{-1} (metal sorbed/biomass) for each trace metals for the three different seawater conditions, and applying these values to Table 1C and carry though for the overall metals associated with *R. iodosum* in Table 1D that accounts for assimilation and adsorption. For all other trace metals and seawater compositions, the yearly metal flux remains robust regardless of the initial seawater composition, as assimilation is the more important process by at least an order of magnitude (see discussion in main text).

Additionally, the model sensitivity to pH was tested and highlighted by examining the amount adsorbed per weight of biomass (μmol mg^{-1}) for mean modern seawater at pH 6.8 and 8 (Figure S1B). In Table S4, we provide the calculation for the number of deprotonated sites at pH 6.8 and 8 and the subsequent calculations at pH 8. At pH 6.8, there are ~1.38 mmol g^{-1} *R. iodosum* of deprotonated carboxyl groups available to adsorb trace metals, as opposed to ~1.56 mmol g^{-1} *R. iodosum* at pH 8. This effectively shows that relative to pH 8, ~88.5% of sites available for trace metal adsorption at pH 8 are deprotonated and adsorbing metals at pH 6.8. In terms of the amount adsorbed per mg biomass, these two scenarios (pH 6.8 and 8) are quite similar for modern seawater (Figure S1B), and this extends to both the simulated Paleoproterozoic seawater and stoichiometrically fixed seawater as well, where the trends at pH 6.8 and 8 mirror one another in terms of the amount of trace metals adsorbed per weight of biomass (μmol mg^{-1}). Based on the limited sensitivity to pH (Figure S1B) and the overall insensitivity in our model to the initial seawater composition once calculations are carried through to total yearly metal fluxes (Figure S2), we consider our calculation of yearly trace metal fluxes to be dominated by assimilation as robust. Therefore, we conclude that our overall calculations (main text Table 1 and Figure 1) are relatively insensitive to reasonable changes in initial seawater composition and pH.

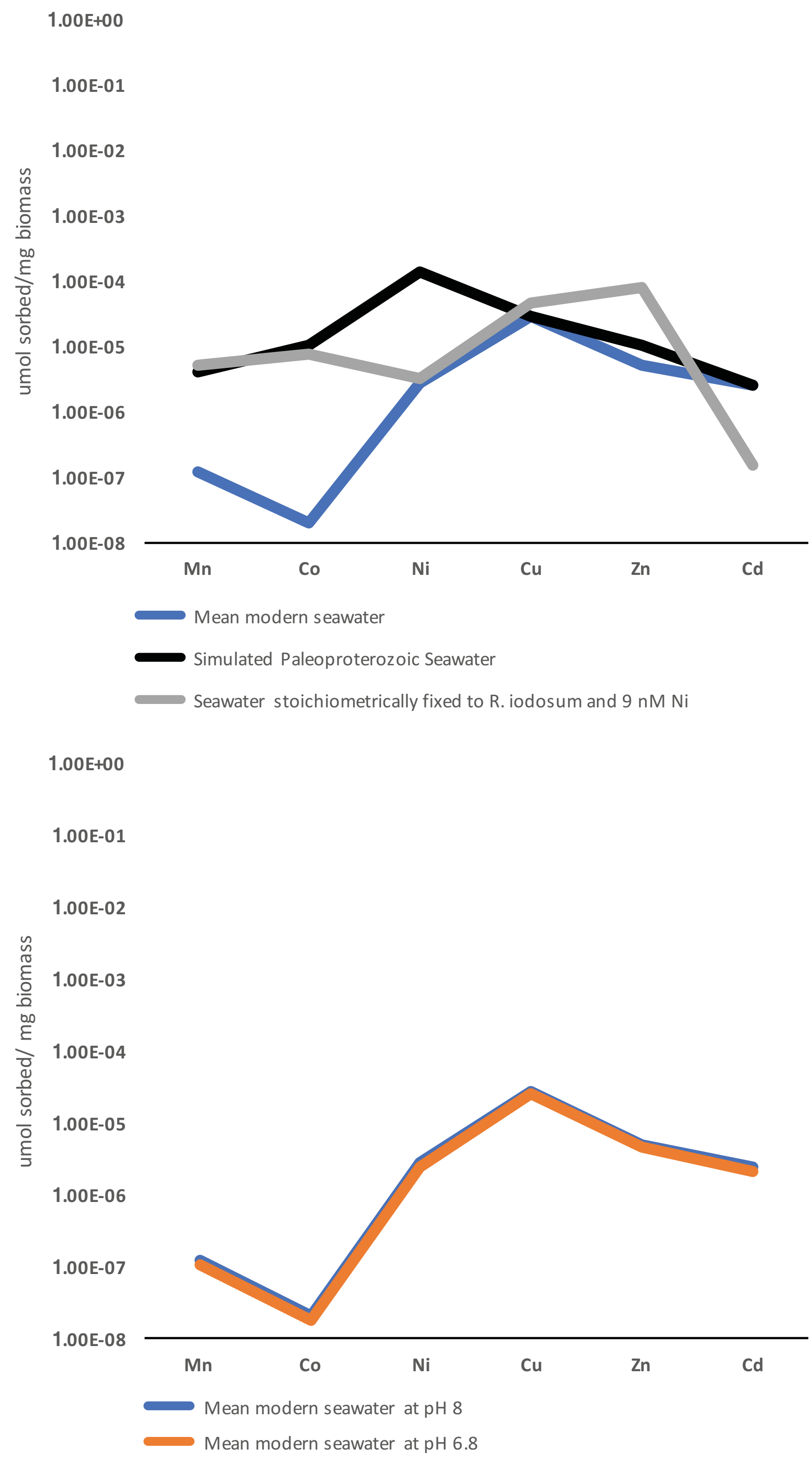

Figure S1: Adsorption calculation sensitivities for (A) differing initial seawater compositions as outlined in Table S2, and (B) the pH at which calculations are performed.

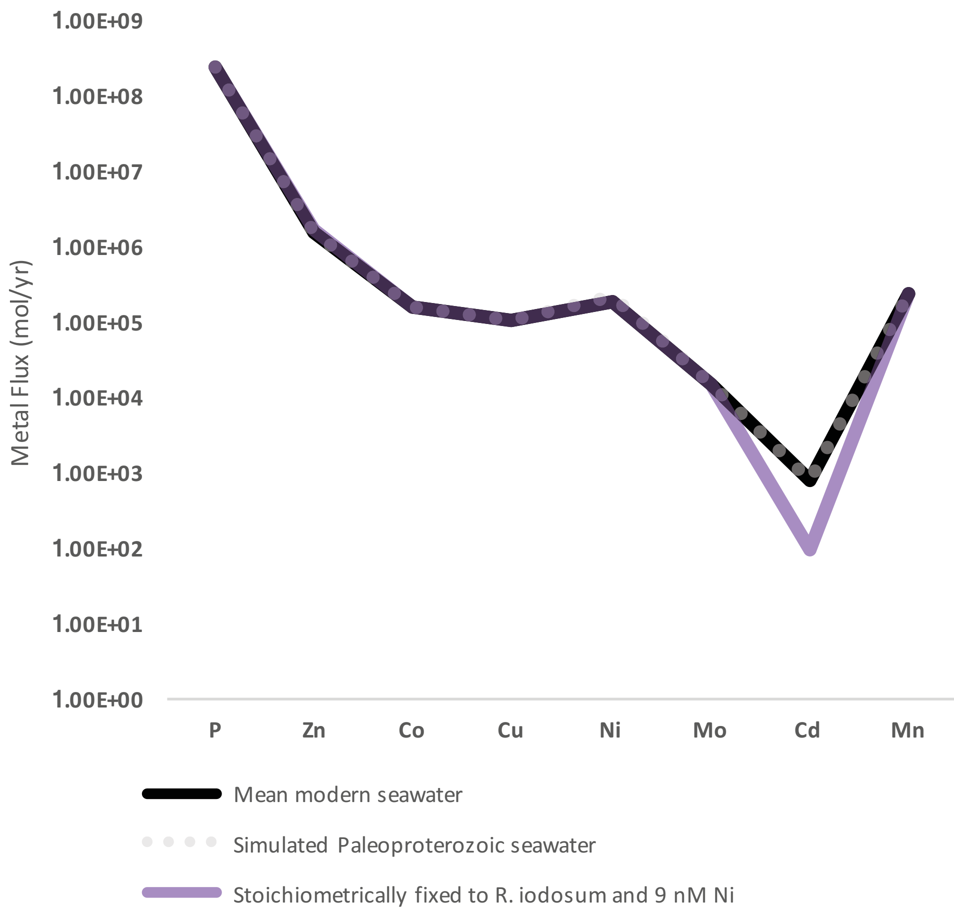

Figure S2: Total yearly fluxes of trace metals (moly yr^{-1}) after main text Figure 1 and Table 1 accounting for the combined affect of assimilation of trace metals by *R. iodosum* and the adsorption calculated for the three initial seawater conditions outlined in Table S2. Note the strong coherence for all trace metals except Cd, which is the least biologically important. Critically, regardless of the initial seawater composition used in adsorption calculations (Table S4), we effectively recreate near identical yearly trace metal fluxes, highlighting that the observed pattern is dominated by bacterial trace metal assimilation and adsorption to the cell surface has only a very minor role.

Table S1. Trace element composition of the Dales Gorge Member, Brockman iron formation (mg kg^{-1})

Source	Sample	P	V	Mn	Co	Cu	Ni	Zn	Mo	Cd	Ti
1	W11 BIF12	2007.4	-	232.3	0.4	0.1	-	5.0	-	0.1	-
1	W13 BIF12	523.7	-	232.3	0.3	-	-	11.0	-	0.1	-
1	W13 BIF12 siderite rich	2880.1	-	464.7	0.7	0.1	-	11.0	-	0.2	-
1	W2 BIF5	872.8	-	309.8	0.8	0.1	-	8.0	-	0.6	-
1	W23 BIF15	1396.4	-	387.2	0.2	-	-	7.0	-	0.1	-
1	W25 BIF15	785.5	-	-	0.2	0.0	-	8.0	-	0.1	-
1	W33 (116-131) BIF16	2880.1	-	309.8	0.3	0.0	-	8.0	0.4	0.1	-
1	W33 (80.5-87) BIF16	1396.4	-	309.8	0.4	0.1	-	10.0	-	0.3	-
1	W35 BIF 16	3665.6	11.0	77.4	0.8	-	-	7.0	-	0.2	-
1	ND85/79(207)BIF14 hem-chert	-	-	-	-	-	-	-	-	-	-
1	ND85/79(207)BIF14 mag-hem	-	-	-	-	-	-	-	-	-	-
1	ND85/79(215.2-215.5m)BIF13	4102.0	-	387.2	-	-	-	7.0	-	-	-
1	W11 (111-132) BIF12	2007.4	-	232.3	-	-	-	5.0	-	-	-
1	W13(107-127)BIF12	523.7	-	232.3	-	-	-	11.0	-	-	-
1	W13(107-127)BIF12	2880.1	-	464.7	-	-	-	11.0	-	-	-
1	W13(107-127)BIF12 sid-chert	-	-	-	-	-	-	-	-	-	-
1	W2(0-16)BIF5	872.8	-	309.8	-	-	-	8.0	-	-	-
1	W23(92-113)BIF15	1396.4	-	387.2	-	-	-	7.0	-	-	-
1	W25(109-129)BIF15	785.5	-	-	-	-	-	8.0	-	-	-
1	W25(109-129)BIF15 mag	-	-	-	-	-	-	-	-	-	-
1	W33(116-131) BIF16*	2880.1	-	309.8	-	-	-	8.0	0.4	-	-
1	W33(32-55)BIF16 mag *CRPG	-	-	-	-	-	-	-	-	-	-
1	W33(80.5-87)BIF16	1396.4	-	309.8	-	-	-	10.0	-	-	-
1	W35(0-15)BIF16	3665.6	-	77.4	-	-	-	7.0	-	-	-
1	W43(44-56)	698.2	-	929.3	-	-	-	8.0	-	-	-
1	ND8585/79 BIF13	4102.0	-	387.2	0.5	-	-	7.0	-	0.1	-
2	DD98-24A	9629.4	19.7	4629.9	29.9	2.6	8.3	18.6	1.2	2.2	513.1
2	DD98-24B	1621.7	10.6	1846.1	7.6	6.8	1.8	8.8	0.5	0.4	355.5
2	DD98-25A	191.2	7.2	2372.7	7.5	2.5	2.0	7.8	0.5	0.7	307.5
2	DD98-26A	6428.3	5.0	518.3	3.0	2.8	0.8	5.6	0.5	0.5	323.9
2	DD98-26B	11601.6	15.6	524.6	9.3	1.3	2.4	11.3	1.1	0.4	650.0
2	DD98-27	85.7	1.6	190.1	1.8	1.1	0.7	-	0.2	-	301.0
2	DD98-28	965.2	37.5	2641.7	69.2	9.2	20.6	50.5	2.3	2.1	314.8
2	DD98-29A	75.9	4.9	143.4	4.4	0.9	2.8	-	0.4	-	289.8
2	DD98-29B	187.9	2.7	98.0	1.0	1.0	0.3	-	0.2	0.2	344.7
2	DD98-30A	720.9	9.7	158.4	10.3	3.3	6.8	10.1	0.8	0.6	319.4
3	DGM-1/B	2474.2	5.7	513.0	-	1.9	1.9	6.8	1.5	-	85.5
3	DGM-1/A	561.7	3.4	234.5	-	2.5	3.0	4.3	4.6	-	121.4
3	DGM-2/A	1266.2	7.2	345.1	-	3.9	3.7	7.7	2.7	-	132.8
3	DGM-2/B	286.1	5.2	455.4	-	1.2	0.8	8.9	1.1	-	77.3
3	DGM-10	102.9	0.6	182.9	-	1.4	1.3	6.2	0.7	-	66.7
3	DGM-3/C	945.8	6.2	-	-	4.5	2.6	7.6	1.5	-	80.3
3	DGM-3/B	495.4	1.8	496.9	-	4.9	3.4	13.8	3.8	-	94.1
3	DGM-3/A	970.0	6.6	1357.9	-	3.9	4.7	10.0	1.7	-	123.0
3	DGM-4	1787.1	3.1	570.7	-	2.1	2.1	13.4	1.9	-	84.5
3	DGM-5	542.7	3.0	356.1	-	2.0	1.6	11.0	1.9	-	77.0
3	DGM-6/B	977.8	5.7	164.7	-	2.6	4.0	29.8	1.7	-	125.8
3	DGM-6/A	1140.8	0.9	494.3	-	2.4	1.4	14.6	2.6	-	82.5
3	DGM-7	1284.2	2.8	871.8	-	1.5	1.6	9.4	1.2	-	78.0
3	DGM-11/B	51.0	1.0	387.1	-	2.1	2.3	16.0	2.6	-	109.8
3	DGM-11/A	153.0	2.1	44.4	-	3.5	2.2	24.6	0.9	-	86.1
3	DGM-17/C	495.1	2.4	1221.8	-	1.4	1.6	39.2	1.9	-	73.3
3	DGM-17/A	3358.7	2.9	2972.0	-	1.6	1.8	12.9	1.4	-	69.9
3	DGM-8/B	1211.7	1.0	217.2	-	1.8	1.4	10.2	1.6	-	66.9
3	DGM-8/A	59.9	0.9	235.5	-	1.3	1.5	8.2	1.6	-	61.2
3	DGM-16/C	8.7	5.4	1094.4	-	2.4	2.2	7.4	1.9	-	119.9
3	DGM-16/B	385.5	7.7	153.0	-	1.2	1.6	36.5	1.0	-	93.1
3	DGM-16/A	413.6	4.0	981.6	-	2.8	2.3	5.5	4.3	-	99.5
4	Dales G. 96.11-12B duplicate	24.8	1.2	118.8	0.3	0.4	-	9.1	0.3	-	-
4	Dales Gorge	15.3	1.4	177.8	0.9	5.3	1.8	14.4	0.3	-	-
4	Dales Gorge 36.075	40.2	1.2	38.4	0.8	1.9	8.1	3.1	0.2	-	-
4	Dales Gorge 36.085	27.2	0.7	49.9	0.7	3.0	5.0	6.9	0.2	-	-
4	Dales Gorge 36.16A	50.8	0.9	164.2	0.3	0.5	-	8.9	0.3	-	-
4	Dales Gorge 36.16B	40.0	0.9	194.0	0.4	0.5	-	9.3	0.3	-	-
4	Dales Gorge 96.10.11	7.7	1.0	28.4	0.3	1.9	2.4	15.5	0.1	-	-
4	Dales Gorge 96.11-12A	22.4	1.1	102.0	0.3	1.2	-	12.0	0.8	-	-
4	Dales Gorge 96.11-12B	24.1	1.2	117.5	0.3	1.0	-	9.2	0.3	-	-
4	Dales Gorge 96.7	14.1	1.5	15.9	0.5	0.5	4.1	4.6	0.2	-	-
5	36_7-9_Hmt1	-	-	20.4	-	-	-	-	-	-	-
5	36_7-9_Hmt10	-	3.3	53.6	-	-	-	-	-	-	52.5
5	36_7-9_Hmt11	-	4.5	38.3	-	-	-	-	-	1.4	8.3
5	36_7-9_Hmt12	-	-	68.6	-	-	-	-	-	-	25.4
5	36_7-9_Hmt13	-	-	1001.8	-	-	-	-	-	-	10.6
5	36_7-9_Hmt14	-	-	54.9	-	7.9	-	-	-	-	9.4
5	36_7-9_Hmt15	545.2	3.9	30.9	-	-	-	-	-	-	15.0
5	36_7-9_Hmt16	440.9	-	43.6	-	-	-	-	-	-	49.8
5	36_7-9_Hmt17	175.2	-	244.8	-	-	10.0	-	-	-	13.8

5	36_7-9_Hmt18	529.9	-	39.1	-	-	-	-	-	-	52.3
5	36_7-9_Hmt19	9474.3	-	6331.7	-	-	-	-	-	-	18.3
5	36_7-9_Hmt2	285.9	-	44.6	-	-	-	19.0	-	3.4	-
5	36_7-9_Hmt20	-	-	30.9	-	-	-	-	-	2.1	11.3
5	36_7-9_Hmt21	-	-	48.0	-	-	-	-	-	-	70.5
5	36_7-9_Hmt21	118.5	2.3	31.5	-	-	1.6	11.2	-	-	24.6
5	36_7-9_Hmt22	536.8	-	5522.6	-	20.0	-	18.3	-	2.8	37.0
5	36_7-9_Hmt23	-	-	21.5	-	-	-	-	0.8	-	17.7
5	36_7-9_Hmt24	269.3	3.5	38.9	1.1	-	-	-	-	-	38.2
5	36_7-9_Hmt25	856.3	-	36.7	-	-	-	-	-	-	9.7
5	36_7-9_Hmt26	953.8	2.2	26.4	-	4.3	-	-	-	-	28.2
5	36_7-9_Hmt27	636.2	-	38.6	-	-	-	-	-	-	22.3
5	36_7-9_Hmt28	776.9	-	53.2	-	-	-	-	-	-	25.5
5	36_7-9_Hmt29	-	-	865.6	-	-	-	-	-	-	32.9
5	36_7-9_Hmt3	131.9	-	57.5	-	-	-	-	-	-	-
5	36_7-9_Hmt30	269.9	4.0	328.9	-	-	-	-	2.0	-	17.6
5	36_7-9_Hmt31	122.3	-	125.3	-	-	4.9	-	-	-	14.3
5	36_7-9_Hmt32	136.3	2.7	145.7	-	-	-	-	-	3.4	44.8
5	36_7-9_Hmt33	-	-	49.3	-	-	-	-	-	-	41.7
5	36_7-9_Hmt34	1415.6	3.6	86.7	1.2	-	-	-	-	-	63.5
5	36_7-9_Hmt35	149.7	-	43.0	-	-	-	10.7	-	-	61.0
5	36_7-9_Hmt36	-	3.9	39.5	-	5.6	47.6	11.5	-	-	27.6
5	36_7-9_Hmt37	-	-	182.1	2.7	-	4.4	-	0.7	-	25.9
5	36_7-9_Hmt38	195.5	-	40.4	1.1	-	-	-	-	1.7	17.4
5	36_7-9_Hmt39	-	-	15.8	-	-	-	-	-	-	12.2
5	36_7-9_Hmt4	-	-	41.8	-	-	-	-	1.7	-	-
5	36_7-9_Hmt40	265.8	-	51.1	-	-	-	-	-	-	51.2
5	36_7-9_Hmt41	-	6.2	-	-	6.7	-	-	0.4	-	18.8
5	36_7-9_Hmt42	-	5.1	47.6	-	-	-	-	-	-	36.3
5	36_7-9_Hmt43	244.5	-	206.7	-	-	-	10.3	-	3.0	59.5
5	36_7-9_Hmt44	-	11.6	86.7	-	-	-	-	-	-	47.5
5	36_7-9_Hmt45	-	5.1	10.2	-	-	-	-	3.7	-	26.9
5	36_7-9_Hmt46	-	3.7	45.9	-	-	-	-	-	-	20.9
5	36_7-9_Hmt47	131.2	3.2	96.5	-	3.7	-	-	-	-	45.9
5	36_7-9_Hmt48	708.1	-	11.1	-	-	-	-	1.6	-	75.4
5	36_7-9_Hmt48	533.4	-	12.7	-	-	-	-	1.4	2.1	32.3
5	36_7-9_Hmt49	569.0	3.6	58.7	-	-	-	-	-	-	47.0
5	36_7-9_Hmt5	273.9	-	49.5	-	-	-	-	-	-	-
5	36_7-9_Hmt50	-	6.0	21.2	-	-	-	14.8	-	-	71.3
5	36_7-9_Hmt51	-	-	46.2	-	-	3.0	-	-	-	65.9
5	36_7-9_Hmt52	-	-	54.8	-	-	-	-	-	-	38.6
5	36_7-9_Hmt53	498.5	4.2	20.7	2.0	-	-	-	-	-	52.2
5	36_7-9_Hmt54	-	-	21.6	-	-	-	17.4	-	-	98.4
5	36_7-9_Hmt55	113.8	-	41.8	-	6.5	-	-	-	-	59.1
5	36_7-9_Hmt56	-	-	92.8	-	-	-	-	-	1.6	70.3
5	36_7-9_Hmt57	1649.8	-	138.9	2.4	-	-	-	-	-	60.0
5	36_7-9_Hmt58	-	-	19.5	-	-	-	-	-	-	70.3
5	36_7-9_Hmt59	201.5	2.8	117.8	-	6.5	11.2	-	-	-	4.5
5	36_7-9_Hmt6	374.1	-	27.1	-	-	-	-	-	-	-
5	36_7-9_Hmt60	217.4	-	19.2	-	-	7.7	-	-	-	91.5
5	36_7-9_Hmt61	-	-	25.2	-	-	-	-	-	-	104.7
5	36_7-9_Hmt62	228.6	-	59.6	-	-	-	-	-	-	89.2
5	36_7-9_Hmt63	-	3.4	26.3	-	4.5	-	-	-	-	217.0
5	36_7-9_Hmt64	-	-	40.9	2.1	-	-	-	-	-	83.8
5	36_7-9_Hmt65	242.8	4.2	65.5	-	-	-	-	-	-	99.0
5	36_7-9_Hmt66	-	-	58.4	-	-	-	-	-	-	127.2
5	36_7-9_Hmt67	631.7	-	142.0	-	-	-	-	-	-	49.4
5	36_7-9_Hmt68	2561.3	-	24.9	-	-	-	-	1.9	-	154.5
5	36_7-9_Hmt69	155.2	3.6	58.8	-	-	-	-	1.4	-	58.2
5	36_7-9_Hmt7	1272.3	-	22.1	-	-	-	-	-	1.5	0.7
5	36_7-9_Hmt8	-	-	34.7	-	-	-	-	2.7	-	-
5	36_7-9_Hmt9	108.3	-	31.1	-	-	-	10.1	-	-	-
5	36_7-9_Mg22	-	-	70.6	-	-	-	-	-	-	68.6
5	36_7-9_Mgt1	1585.1	-	16.9	-	-	-	-	-	-	-
5	36_7-9_Mgt10	585.0	-	8.3	-	-	-	-	-	-	17.8
5	36_7-9_Mgt11	-	-	26.4	-	-	-	-	0.6	-	42.3
5	36_7-9_Mgt12	553.0	-	244.6	1.7	-	2.9	-	-	-	15.9
5	36_7-9_Mgt12	374.5	-	328.5	-	-	-	-	-	-	13.9
5	36_7-9_Mgt13	68.9	2.6	44.0	-	-	-	-	-	1.5	23.8
5	36_7-9_Mgt14	308.0	2.6	31.5	-	10.8	-	-	-	-	14.6
5	36_7-9_Mgt15	257.7	1.8	9.2	-	-	-	6.9	0.3	-	16.9
5	36_7-9_Mgt16	64.1	1.6	9.8	-	-	-	-	2.9	-	25.9
5	36_7-9_Mgt17	83.8	-	11.7	-	-	-	-	-	-	17.5
5	36_7-9_Mgt18	119.5	-	12.9	0.8	-	3.7	-	1.3	-	14.8
5	36_7-9_Mgt19	380.6	2.3	20.0	0.8	-	-	5.7	1.7	-	33.1
5	36_7-9_Mgt2	2871.0	-	24.3	-	5.0	-	-	-	-	6.5
5	36_7-9_Mgt20	-	2.7	17.3	-	-	-	-	-	-	27.1
5	36_7-9_Mgt21	-	-	11.8	-	-	-	21.5	-	-	18.3
5	36_7-9_Mgt23	-	-	11.4	-	-	-	-	-	3.0	60.0
5	36_7-9_Mgt23	524.1	-	52.9	-	-	-	-	-	-	156.0

5	36_7-9_Mgt24	300.6	2.7	36.7	-	-	1.9	-	-	-	87.2
5	36_7-9_Mgt25	1921.3	-	140.4	-	-	-	-	-	-	110.7
5	36_7-9_Mgt3	1590.6	-	19.1	1.3	5.3	-	-	-	-	5.3
5	36_7-9_Mgt33	-	-	1588.7	-	-	-	-	-	-	115.3
5	36_7-9_Mgt4	128.2	2.7	11.8	-	-	-	-	-	2.5	83.5
5	36_7-9_Mgt5	-	-	13.3	-	-	-	29.5	-	-	7.8
5	36_7-9_Mgt6	122.0	-	20.5	-	-	-	-	-	-	138.5
5	36_7-9_Mgt7	423.3	2.8	19.2	-	-	-	-	-	-	25.2
5	36_7-9_Mgt8	111.0	-	13.6	-	-	-	-	-	-	127.4
5	36_7-9_Mgt9	239.9	-	24.1	-	-	-	-	-	-	200.6
5	36.10-1	14.6	-	3.3	-	-	-	-	-	-	80.8
5	36.10-hmt-1	31.1	2.3	64.1	-	-	-	2.0	-	-	43.9
5	36.10-hmt-2	29.5	0.3	22.2	-	-	-	-	-	-	63.0
5	36.10-Hmt1	48.7	1.3	48.2	-	-	-	-	-	-	66.3
5	36.10-Hmt10	47.6	1.9	62.8	0.7	-	-	-	-	-	45.5
5	36.10-Hmt11	121.6	3.6	105.7	0.6	4.3	-	4.2	1.5	-	39.4
5	36.10-Hmt2	5.3	-	7.0	-	-	-	-	-	-	46.6
5	36.10-Hmt3	501.9	4.0	133.8	-	-	-	7.0	1.4	-	66.0
5	36.10-Hmt4	34.2	0.9	33.0	-	-	-	-	0.3	0.2	68.6
5	36.10-Hmt5	73.1	1.3	44.9	-	-	-	2.2	0.3	-	77.5
5	36.10-Hmt6	141.2	2.3	109.5	-	-	-	4.4	-	-	-
5	36.10-Hmt6	82.6	-	76.0	-	-	-	-	-	-	-
5	36.10-Hmt7	2.8	0.1	2.3	-	-	-	-	-	-	-
5	36.10-Hmt8	148.5	0.5	27.1	-	0.9	-	-	-	-	733.4
5	36.10-Hmt9	551.8	1.0	68.0	-	-	-	2.1	0.9	-	677.1
5	36.10-Mgt1	31.1	0.4	12.2	-	-	-	0.7	-	-	31.5
5	36.10-Mgt10	297.7	1.1	53.8	-	-	-	-	1.0	-	78.5
5	36.10-Mgt11	127.4	5.7	136.5	-	-	-	3.7	1.9	-	160.5
5	36.10-Mgt2	89.1	1.2	38.9	-	-	-	-	-	-	71.0
5	36.10-Mgt3	41.4	2.3	50.9	-	48.5	-	1.2	0.3	0.1	76.9
5	36.10-Mgt4	132.5	4.1	133.4	-	-	-	4.6	-	-	101.4
5	36.10-Mgt5	810.9	2.4	104.5	-	-	-	-	0.5	-	82.1
5	36.10-Mgt6	1562.8	2.3	77.3	-	-	-	2.9	1.1	-	114.9
5	36.10-Mgt7	73.8	2.5	67.5	-	-	-	-	0.2	-	72.5
5	36.10-Mgt8	33.8	0.2	7.3	-	-	-	0.7	-	-	63.4
5	36.10-Mgt9	53.7	2.3	64.1	-	-	-	1.9	-	-	67.4
5	96.12hmt-1	-	-	6.9	-	-	-	-	-	-	31.0
5	96.12hmt-10	9.4	-	5.1	-	-	-	-	-	-	54.0
5	96.12hmt-11	-	2.4	1.9	-	-	-	-	-	-	26.4
5	96.12hmt-12	-	-	32.0	-	-	-	-	-	-	25.0
5	96.12hmt-13	-	-	1.2	-	-	-	-	0.2	-	363.6
5	96.12hmt-14	-	-	4.2	-	-	-	-	-	-	65.6
5	96.12hmt-15	-	-	6.6	-	-	-	-	-	-	55.8
5	96.12hmt-16	-	-	6.6	-	-	-	-	-	-	34.3
5	96.12hmt-17	-	-	16.8	-	-	-	-	-	-	32.7
5	96.12hmt-18	-	-	41.8	-	-	-	-	-	-	33.5
5	96.12hmt-19	460.9	-	79.9	-	30.0	-	325.9	-	2.5	28.6
5	96.12hmt-2	-	-	1.0	-	-	-	-	-	-	23.9
5	96.12hmt-3	-	-	10.6	-	-	-	-	-	-	32.5
5	96.12hmt-4	-	-	0.8	-	-	-	5.2	-	-	164.3
5	96.12hmt-5	103.4	8.0	9.8	-	-	-	-	-	2.8	38.3
5	96.12hmt-6	120.0	-	19.3	-	-	-	-	-	-	31.2
5	96.12hmt-7	-	-	22.5	-	-	-	-	-	-	114.4
5	96.12hmt-8	-	12.2	24.7	-	-	-	-	-	-	31.1
5	96.12hmt-9	191.0	-	9.6	-	-	-	-	-	-	36.2
5	96.12mgt-1	-	-	1.9	-	-	-	-	-	-	65.4
5	96.12mgt-10	-	-	0.3	-	0.3	-	-	-	-	10.1
5	96.12mgt-11	-	-	0.3	-	-	-	-	-	-	9.6
5	96.12mgt-12	-	-	-	-	-	-	5.5	-	-	19.4
5	96.12mgt-13	-	-	3.0	-	-	-	-	-	-	16.4
5	96.12mgt-14	-	-	-	-	-	-	-	-	-	12.3
5	96.12mgt-15	-	-	-	-	-	-	-	-	-	5.8
5	96.12mgt-16	-	-	14.1	-	-	-	-	-	-	6.0
5	96.12mgt-17	-	-	1.6	-	-	-	-	-	-	3.3
5	96.12mgt-18	-	-	13.2	-	-	-	-	-	-	8.9
5	96.12mgt-19	-	-	8.7	-	-	-	-	-	-	13.6
5	96.12mgt-2	-	-	0.6	-	-	-	-	-	-	105.9
5	96.12mgt-20	-	-	0.2	-	-	-	-	-	-	8.7
5	96.12mgt-21	44.3	-	2.4	-	-	-	-	-	-	14.6
5	96.12mgt-22	-	-	0.6	-	-	-	-	-	-	6.1
5	96.12mgt-23	-	-	-	-	-	-	-	-	0.2	-
5	96.12mgt-24	67.5	-	-	-	-	-	-	-	-	-
5	96.12mgt-25	-	-	0.5	-	-	-	0.2	-	-	3.0
5	96.12mgt-26	-	-	2.5	-	-	-	-	-	0.2	11.1
5	96.12mgt-27	-	-	6.4	-	-	-	-	-	-	-
5	96.12mgt-28	-	-	-	-	-	-	-	-	-	-
5	96.12mgt-29	-	-	4.5	0.7	-	-	-	1.0	-	0.6
5	96.12mgt-3	-	-	1.0	-	-	-	-	-	-	44.3
5	96.12mgt-30	-	-	-	-	-	-	-	-	-	-
5	96.12mgt-31	-	-	2.5	-	-	-	-	-	-	-

5	96.12mgt-32	238.7	-	11.3	2.4	-	-	-	-	-	-
5	96.12mgt-33	-	11.2	18.3	-	-	-	-	-	-	-
5	96.12mgt-34	-	0.2	1.8	-	-	-	-	-	-	-
5	96.12mgt-35	-	-	0.6	-	-	-	0.5	-	-	-
5	96.12mgt-36	-	8.0	6.3	-	-	-	-	-	-	0.4
5	96.12mgt-37	1.2	-	0.1	-	-	-	0.2	-	-	-
5	96.12mgt-39	-	3.7	2.4	-	-	-	-	0.9	-	-
5	96.12mgt-4	215.5	-	7.4	4.1	-	-	-	-	-	16.7
5	96.12mgt-40	-	-	1.0	-	-	-	-	-	-	-
5	96.12mgt-41	-	6.1	8.1	-	-	-	-	-	-	-
5	96.12mgt-42	-	-	4.8	-	-	-	-	-	-	-
5	96.12mgt-43	-	-	-	-	-	-	-	-	-	-
5	96.12mgt-44	-	-	2.2	-	-	-	0.9	-	-	-
5	96.12mgt-45	180.0	-	10.2	-	-	-	-	-	-	14.2
5	96.12mgt-46	22.5	-	15.8	-	-	-	-	-	-	2.7
5	96.12mgt-47	-	-	23.1	-	-	-	-	-	-	-
5	96.12mgt-48	-	-	6.5	-	-	-	-	-	-	-
5	96.12mgt-49	-	-	1.7	-	-	-	-	-	-	-
5	96.12mgt-5	-	-	0.8	-	-	-	-	-	-	9.9
5	96.12mgt-50	-	-	1.2	-	-	-	-	-	-	-
5	96.12mgt-51	-	-	1.9	-	-	-	-	-	-	-
5	96.12mgt-52	4.0	-	6.0	-	-	-	-	-	-	-
5	96.12mgt-53	-	-	0.3	-	-	-	0.6	0.1	-	-
5	96.12mgt-6	-	-	0.8	-	-	-	-	-	-	11.4
5	96.12mgt-7	-	-	3.0	-	-	-	0.9	-	-	27.3
5	96.12mgt-8	116.1	-	5.6	-	-	-	-	2.2	-	26.6
5	96.12mgt-9	-	-	11.8	4.4	-	-	-	-	-	20.4
Bulk analyses (n=68)	average	1467.7	5.0	563.8	5.1	2.1	3.2	11.4	1.3	0.5	179.0
	n=	63	43	60	30	48	37	60	44	18	32
	1 std dev	2130.5	6.5	811.7	13.4	1.8	3.5	8.5	1.1	0.6	147.4
Laser ablation (n=196)	average	480.0	3.4	121.1	1.8	10.1	9.0	16.1	1.2	1.9	57.2
	n=	101	63	187	17	17	11	35	32	19	160
	1 std dev	1043.6	2.5	626.2	1.2	12.2	13.2	54.4	0.9	1.1	87.2
All data (n=264)	average	859.40	4.06	228.63	3.90	4.18	4.50	13.12	1.24	1.21	77.47
	maximum	11601.64	37.51	6331.73	69.19	48.52	47.58	325.87	4.62	3.35	733.41
	minimum	1.22	0.08	0.08	0.21	0.03	0.34	0.18	0.09	0.06	0.44
	n=	164	106	247	47	65	48	95	76	37	192
	1 std dev	1620.8	4.6	700.5	10.8	7.2	7.2	33.5	1.0	1.1	109.2

1. Bulk analysis (drillcore from Alibert and McCulloch, 1993)
2. Bulk analysis (drillcore DD98SGP001, this study) †
3. Bulk analysis (drillecore DDH-47A*, this study) †
4. Bulk analysis (drillcore DDH-44, Pecoits et al., 2009; Konhauser et al., 2009; 2011)
5. Laser ablation (drillcore DDH-44, Pecoits et al., 2009; Konhauser et al., 2009; 2011)

† For trace element analysis, ~50 mg of each sample was digested sequentially in conc. HF-HNO3, aqua regia, and 6M HCl and analyzed for trace element concentrations in 2% HNO3 with In as an internal standard using a Thermo Scientific Element2 High Resolution Inductively Coupled Plasma Mass Spectrometer. The instrument was calibrated with multi-element solutions and the results verified against geostandards BHVO-2, IF-G, and GL-O treated in the same batch.

Table S2. Composition of initial seawater water values used for adsorption calculations

	Mn	Co	Ni	Cu	Zn	Cd
Mean modern seawater (M)*	3.00E-10	2.00E-11	8.00E-09	3.00E-09	5.00E-09	6.00E-10
Simulated Paleoproterozoic seawater (M)**	1.00E-08	1.00E-08	4.00E-07	3.00E-09	1.00E-08	6.00E-10
Seawater stoichiometrically fixed to *R. iodosum* and 9 nM Ni (M)***	1.20E-08	7.57E-09	9.00E-09	4.98E-09	7.80E-08	3.76E-11

*Bruland and Lohan (2003)

**Simulated values set at Paleoproterozoic estimates for: Mn (Saito et al., 2003), Co (Saito et al., 2003; Swanner et al., 2014) and, Ni (Konhauser et al., 2009); Cu (Chi Fru et al., 2016); Zn (Robbins et al., 2013; Scott et al., 2013), Cd set at modern.

***Fixed to the stoichiometry of *R. iodosum* and 9 nM Ni after Konhauser et al. (2009)

Table S3. Concentrations of metals in *Rhodovulum iodense* biomass by dry weight (mg Me g^{-1} dry weight) measured by ICP-MS.

Sample	Replicate	P	Mo*	Mn	Fe	Co	Ni	Cu	Zn
0.5X metal	A	11.372	0.000	0.015	0.297	0.003	0.018	0.007	0.052
	B	16.891	BD	0.022	1.335	0.015	0.020	0.010	0.139
	C	39.598	0.001	0.053	4.085	0.038	0.058	0.027	0.398
1X metal	A	29.183	BD	0.048	2.675	0.026	0.039	0.020	0.233
	B	23.909	0.001	0.045	2.402	0.031	0.032	0.020	0.397
	C	24.883	0.009	0.044	2.563	0.035	0.038	0.020	0.427
	average	25.992	0.005	0.045	2.547	0.031	0.036	0.020	0.352
2X metal	A	31.284	0.002	0.058	4.134	0.045	0.039	0.024	0.506
	B	27.909	0.002	0.166	12.899	0.066	0.040	0.051	1.809
	C	33.497	0.001	0.195	15.591	0.071	0.043	0.063	2.270
5X metal	A	54.028	0.005	0.251	14.486	0.110	0.057	0.071	2.573
	B	1.022	0.006	0.060	101.600	0.034	0.012	0.008	0.074
	C	2.237	0.004	0.043	61.449	0.024	0.008	0.006	0.052

Table S4. Adsorption calculations for mean modern, simulated Paleoproterozoic, and seawater stoichiometrically fixed to *R. iodosum* and 9 nM Ni.

A) Deprotonation calculations

pKa from Martinez et al. (2016)	site concentration (mmol g^{-1})	ratio of L- to HL at pH 6.8	Percent of sites deprotnated at pH 6.8 (%)	Deprotonated site concentration at pH 6.8 (mmol g^{-1})	ratio of L- to HL at pH 8	Percent of sites deprotnated at pH 8 (%)	Deprotonated site concentration at pH 8 (mmol g^{-1})
4.85	0.57	89.13	98.89	0.56	1412.54	99.93	0.57
6.15	1.00	4.47	81.71	0.82	70.79	98.61	0.99
7.75	0.73	0.11	10.09	0.07	1.78	64.01	0.47
9.20	0.55	0.00	0.40	0.00	0.06	5.94	0.03
Max binding sites (mmol g^{-1})	2.85			1.46			2.06
Percent of site deprotonated (%)				51.11			72.12

B) Adsorption with modern seawater

	Mn	Co	Ni	Cu	Zn	Cd
>COO- sites at pH 8 (mmol g^{-1})	1.56	1.56	1.56	1.56	1.56	1.56
>COO- sites at pH 8 (mol kg^{-1} seawater)	4.46E-08	4.46E-08	4.46E-08	4.46E-08	4.46E-08	4.46E-08
Acetate-metal log K (Martell and Smith, 1977)	0.80	1.10	0.74	1.83	1.10	1.56
Adjusted metal log K (Fein et al., 2001)	2.42	2.81	2.34	3.77	2.81	3.41
Adjusted metal K (Fein et al., 2001)	261.82	647.14	218.47	5851.94	647.14	2591.79
Bruland and Lohan (2003) mean seawater concentration (mol kg^{-1})	3.00E-10	2.00E-11	8.00E-09	3.00E-09	5.00E-09	6.00E-10
>COO-M (mol kg^{-1} (complex/seawater))	3.50E-15	5.77E-16	7.79E-14	7.82E-13	1.44E-13	6.93E-14
mg kg^{-1} (bacteria/seawater)	0.02865	0.02865	0.02865	0.02865	0.02865	0.02865
umol mg^{-1} (metal/biomass)	1.22E-07	2.01E-08	2.72E-06	2.73E-05	5.03E-06	2.42E-06

Sum of trace metal concentrations (mol kg^{-1})	1.69E-08
Number of carboxyl sites (mol kg^{-1})	4.46E-08
Sum of occupied binding sites (>COO-M; mol kg^{-1}):	1.08E-12
Percent of carboxyl groups ocupied (%):	0.002

C) Adsorption with simulated Paleoproterozoic seawater

	Mn	Co	Ni	Cu	Zn	Cd
>COO- sites at pH 8 (mmol g^{-1})	1.56	1.56	1.56	1.56	1.56	1.56
>COO- sites at pH 8 (mol kg^{-1} seawater)	4.46E-08	4.46E-08	4.46E-08	4.46E-08	4.46E-08	4.46E-08
Acetate-metal log K (Martell and Smith, 1977)	0.8	1.1	0.74	1.83	1.1	1.56
Adjusted metal log K (Fein et al., 2001)	2.42	2.81	2.34	3.77	2.81	3.41
Adjusted metal K (Fein et al., 2001)	261.82	647.14	218.47	5851.94	647.14	2591.79
Simulated Paleoproterozoic seawater (mol kg^{-1})	1.00E-08	1.00E-08	4.00E-07	3.00E-09	1.00E-08	6.00E-10
>COO-M (mol kg^{-1} (complex/seawater))	1.17E-13	2.88E-13	3.89E-12	7.82E-13	2.88E-13	6.93E-14
mg kg^{-1} (bacteria/seawater)	0.02865	0.02865	0.02865	0.02865	0.02865	0.02865
umol mg^{-1} (metal/biomass)	4.07E-06	1.01E-05	1.36E-04	2.73E-05	1.01E-05	2.42E-06

Sum of trace metal concentrations (mol kg^{-1})	4.34E-07
Number of carboxyl sites (mol kg^{-1})	4.46E-08
Sum of occupied binding sites (>COO-M; mol kg^{-1}):	5.44E-12
Percent of carboxyl groups ocupied (%):	0.012

D) Adsoprtion with seawater stoichiometrically fixed to R. iodosum and 9 nM Ni

	Mn	Co	Ni	Cu	Zn	Cd
>COO- sites at pH 8 (mmol g^{-1})	1.56	1.56	1.56	1.56	1.56	1.56
>COO- sites at pH 8 (mol kg^{-1} seawater)	4.46E-08	4.46E-08	4.46E-08	4.46E-08	4.46E-08	4.46E-08
Acetate-metal log K (Martell and Smith, 1977)	0.8	1.1	0.74	1.83	1.1	1.56
Adjusted metal log K (Fein et al., 2001)	2.42	2.81	2.34	3.77	2.81	3.41
Adjusted metal K (Fein et al., 2001)	261.82	647.14	218.47	5851.94	647.14	2591.79
Seawater stoichiometrically fixed to R. iodosum and 9 nM Ni (mol kg^{-1})	1.20E-08	7.57E-09	9.00E-09	4.98E-09	7.80E-08	3.76E-11
>COO-M (mol kg^{-1} (complex/seawater))	1.40E-13	2.18E-13	8.76E-14	1.30E-12	2.25E-12	4.34E-15
mg kg^{-1} (bacteria/seawater)	0.02865	0.02865	0.02865	0.02865	0.02865	0.02865
umol mg^{-1} (metal/biomass)	4.88E-06	7.62E-06	3.06E-06	4.53E-05	7.86E-05	1.52E-07

Sum of trace metal concentrations (mol kg^{-1})	1.12E-07
Number of carboxyl sites (mol kg^{-1})	4.46E-08
Sum of occupied binding sites (>COO-M; mol kg^{-1}):	4.00E-12
Percent of carboxyl groups ocupied (%):	0.009

Table S5. Trace element contribution from average marine phytoplankton

	P	Zn	Co	Cu	Ni	Mo	Cd	Mn
single-cell concentration (mol L^{-1})	1.20E-01	8.00E-05	2.40E-05	3.50E-05	*n.d.*	3.10E-06	1.70E-05	4.20E-04
cell volume (um^3)	100	100	100	100	100	100	100	100
cell volume (L)	1.00E-13	1.00E-13	1.00E-13	1.00E-13	1.00E-13	1.00E-13	1.00E-13	1.00E-13
single-cell metal quantity (moles)	1.20E-14	8.00E-18	2.40E-18	3.50E-18	*n.d.*	3.10E-19	1.70E-18	4.20E-17
minimum number of cells needed to form BIF	4.50E+20	4.50E+20	4.50E+20	4.50E+20	4.50E+20	4.50E+20	4.50E+20	4.50E+20
annual biomass contribution (mol yr^{-1})	5.40E+06	3.60E+03	1.08E+03	1.58E+03	*n.d.*	1.40E+02	7.65E+02	1.89E+04
average amount in BIF layer (mol yr^{-1})	2.90E+09	2.10E+07	6.91E+06	6.87E+06	8.00E+06	1.35E+06	1.12E+06	4.34E+08
relative to BIF	1.86E-03	1.72E-04	1.56E-04	2.29E-04	*n.d.*	1.03E-04	6.81E-04	4.35E-05

Trace element data from Ho et al. (2003)

Table S6. Trace elements associated with contributions from continental crust and hydrothermal emissions.

	P	Zn	Co	Cu	Ni	Mo	Cd	Mn	Ti
Average crust concentration* (mol kg^{-1})	1.07E-02	1.02E-03	2.94E-04	4.41E-04	8.01E-04	1.15E-05	8.01E-07	1.41E-02	8.01E-02
Crustal contribution (mol yr^{-1}) based on average Ti in the Dales Gorge Member (0.0016 mol kg^{-1})	2.24E+07	2.15E+06	6.17E+05	9.26E+05	1.68E+06	2.41E+04	1.68E+03	2.96E+07	1.60E-03
Global high-temp. hydrothermal fluid flux** (mol yr^{-1})	4.50E+07	3.20E+09	6.80E+06	1.30E+09				3.40E+10	
Global high-temp. hydrothermal fluid flux scaled to the Hamersley basin photic zone (mol yr^{-1})	3.46E+02	2.46E+04	5.23E+01	1.00E+04				2.62E+05	

*Rudnick and Gao (2003)

**Elderfield and Schultz (1996)

REFERENCES CITED

Alibert, C., and McCulloch, M., 1993, Rare earth element and neodymium isotopic compositions of the banded iron-formations and associated shales from Hamersley, western Australia: Geochimica et Cosmochimica Acta, v. 57, p. 187–204.

Bruland, K.W., and Lohan, M.C., 2003, Controls of trace metals in seawater, *in* Holland, H.D. and Turekian, K. eds., Treatise on Geochemistry, Elsevier, v. 6, p. 23–47, doi: 10.1016/b0-08-043751-6/06105-3.

Chi Fru, E., Rodríguez, N.P., Partin, C.A., Lalonde, S.V., Andersson, P.S., Weiss, D.J., Albani, A.E., Rodushkin, I., and Konhauser, K.O., 2016, Cu isotopes in marine black shales record the Great Oxidation Event: Proceedings of the National Academy of Sciences, v. 113, no. 18, p. 4941–4946, doi: 10.1073/pnas.1523544113.

Elderfield, H., and Schultz, A., 1996, Mid-ocean ridge hydrothermal fluxes and the chemical composition of the ocean: Annual Review of Earth and Planetary Sciences, v. 24, p. 191-224.

Fein, J., Martin, A., and Wightman, P., 2001, Metal adsorption onto bacterial surfaces: Development of a predictive approach: Geochimica et Cosmochimica Acta, v. 65, p. 4267–4273.

Ho, T.Y., Quigg, A., Finkel, Z.V., Milligan, A.J., Wyman, K., Falkowski, P.G., and Morel, F.M.M., 2003, The elemental composition of some marine phytoplankton: Journal of Phycology, v. 39, p. 1145–1159, doi: 10.1111/j.0022-3646.2003.03-090.x.

Konhauser, K.O., Pecoits, E., Lalonde, S.V., Papineau, D., Nisbet, E.G., Barley, M.E., Arndt, N.T., Zahnle, K., and Kamber, B.S., 2009, Oceanic nickel depletion and a methanogen famine before the Great Oxidation Event: Nature Geoscience, v. 458, p. 750–753, doi: 10.1038/nature07858.

Konhauser, K.O., Lalonde, S.V., Planavsky, N.J., Pecoits, E., Lyons, T.W., Mojzsis, S.J., Rouxel, O.J., Barley, M.E., Rosière, C.A., Fralick, P.W., Kump, L.R., and Bekker, A., 2011, Aerobic bacterial pyrite oxidation and acid rock drainage during the Great Oxidation Event: Nature Geoscience, v. 478, p. 369–373, doi: 10.1038/nature10511.

Martell, A. E., Smith, R. M., 1977, *Critical Stability Constants*, Vol. 3, Other Organic Ligands, Plenum, New York, NY.

Martinez, R.E., Konhauser, K.O., Paunova, N., Wu, W., Alessi, D.S., and Kappler, A., 2016, Surface reactivity of the anaerobic phototrophic Fe(II)-oxidizing bacterium *Rhodovulum iodosum*: implications for trace metal budgets in ancient oceans and banded iron formations: Chemical Geology, v. 442, p. 113-120, doi: 10.1016/j.chemgeo.2016.009.004.

Pecoits, E., Gingras, M.K., Barley, M.E., Kappler, A., Posth, N., and Konhauser, K.O., 2009, Petrography and geochemistry of the Dales Gorge banded iron formation: Paragenetic sequence, source and implications for palaeo-ocean chemistry: Precambrian Research, v. 172, p. 163–187.

Robbins, L.J., Lalonde, S.V., Saito, M.A., Planavsky, N.J., Mloszewska, A.M., Pecoits, E., Scott, C., Dupont, C.L., Kappler, A., and Konhauser, K.O., 2013, Authigenic iron oxide proxies for marine zinc over geological time and implications for eukaryotic metallome evolution: Geobiology, v. 11, p. 295-306.

Rudnick, R.L., and Gao, S., 2003, The composition of the continental crust: Treatise on Geochemistry v. 3, p. 1-64.

Saito, M.A., Sigman, D.M, and Morel, F.M.M., 2003, The bioinorganic chemistry of the ancient ocean: the co-evolution of cyanobacterial metal requirements and biogeochemical cycles at the Archean-Proterozoic boundary?: Inorganica Chimica Acta, v. 356, p. 308-318.

Scott, C.T., Planavsky, N.J., Dupont, C.L., Kendall, B., Gill, B.C., Robbins, L.J., Husband, K.F., Arnold, G.L., Wing, B.A., Poulton, S.W., Bekker, A., Anbar, A.D., Konhauser, K.O., and Lyons, T.W., 2013, Bioavailability of zinc in marine systems through time: Nature Geosciences, v. 6, p. 125-128.

Swanner, E.D., Planavsky, N., Lalonde, S.V., Robbins, L.J., Bekker, A., Rouxel, O., Saito, M.A., Kappler, A., Mojzsis, S.J., and Konhauser, K.O., 2014, Cobalt and marine redox evolution: Earth and Planetary Science Letters, v. 390, p. 253-263.